OXFORD | human reproduction

Early pregnancy

Morphologic development of the first-trimester utero-placental vasculature is positively associated with embryonic and fetal growth: the Rotterdam Periconception Cohort

E.S. De Vos [1], A.G.M.G.J. Mulders [1,*], A.H.J. Koning [2], S.P. Willemsen [1,3], M. Rousian [1], B.B. Van Rijn [1], E.A.P. Steegers [1], and R.P.M. Steegers-Theunissen [1]

[1]Department of Obstetrics and Gynecology, Erasmus MC University Medical Center, Rotterdam, The Netherlands
[2]Department of Pathology, Erasmus MC University Medical Center, Rotterdam, The Netherlands
[3]Department of Biostatistics, Erasmus MC University Medical Center, Rotterdam, The Netherlands

*Correspondence address. Department of Obstetrics and Gynecology/Periconception Epidemiology, Erasmus MC University Medical Center, PO Box 2040, 3000 CA Rotterdam, The Netherlands. Tel: +31-10-7033492/+31-6-28914348; Fax: +31-10 7036815; E-mail: a.mulders@erasmusmc.nl https://orcid.org/0000-0002-4407-8323

ABSTRACT

STUDY QUESTION: Is morphologic development of the first-trimester utero-placental vasculature associated with embryonic growth and development, fetal growth, and birth weight percentiles?

SUMMARY ANSWER: Using the utero-placental vascular skeleton (uPVS) as a new imaging marker, this study reveals morphologic development of the first-trimester utero-placental vasculature is positively associated with embryonic growth and development, fetal growth, and birth weight percentiles.

WHAT IS KNOWN ALREADY: First-trimester development of the utero-placental vasculature is associated with placental function, which subsequently impacts embryonic and fetal ability to reach their full growth potential. The attribution of morphologic variations in the utero-placental vascular development, including the vascular structure and branching density, on prenatal growth remains unknown.

STUDY DESIGN, SIZE, DURATION: This study was conducted in the VIRTUAL Placental study, a subcohort of 214 ongoing pregnancies, embedded in the prospective observational Rotterdam Periconception Cohort (Predict study). Women were included before 10 weeks gestational age (GA) at a tertiary referral hospital in The Netherlands between January 2017 and March 2018.

PARTICIPANTS/MATERIALS, SETTING, METHODS: We obtained three-dimensional power Doppler volumes of the gestational sac including the embryo and the placenta at 7, 9, and 11 weeks of gestation. Virtual Reality-based segmentation and a recently developed skeletonization algorithm were applied to the power Doppler volumes to generate the uPVS and to measure utero-placental vascular volume (uPVV). Absolute vascular morphology was quantified by assigning a morphologic characteristic to each voxel in the uPVS (i.e. end-, bifurcation-crossing-, or vessel point). Additionally, total vascular length (mm) was calculated. The ratios of the uPVS characteristics to the uPVV were calculated to determine the density of vascular branching. Embryonic growth was estimated by crown-rump length and embryonic volume. Embryonic development was estimated by Carnegie stages. Fetal growth was measured by estimated fetal weight in the second and third trimester and birth weight percentiles. Linear mixed models were used to estimate trajectories of longitudinal measurements. Linear regression analysis with adjustments for confounders was used to evaluate associations between trajectories of the uPVS and prenatal growth. Groups were stratified for conception method (natural/IVF-ICSI conceptions), fetal sex (male/female), and the occurrence of placenta-related complications (yes/no).

MAIN RESULTS AND THE ROLE OF CHANCE: Increased absolute vascular morphologic development, estimated by positive random intercepts of the uPVS characteristics, is associated with increased embryonic growth, reflected by crown-rump length (endpoints $\beta = 0.017$, 95% CI [0.009; 0.025], bifurcation points $\beta = 0.012$, 95% CI [0.006; 0.018], crossing points $\beta = 0.017$, 95% CI [0.008; 0.025], vessel points $\beta = 0.01$, 95% CI [0.002; 0.008], and total vascular length $\beta = 0.007$, 95% CI [0.003; 0.010], and similarly with embryonic volume and Carnegie stage, all *P*-values ≤ 0.01. Density of vascular branching was negatively associated with estimated fetal weight in the third trimester (endpoints: uPVV $\beta = -94.972$, 95% CI [−185.245; −3.698], bifurcation points: uPVV $\beta = -192.601$ 95% CI [−360.532; −24.670]) and birth weight percentiles (endpoints: uPVV $\beta = -20.727$, 95% CI [−32.771; −8.683], bifurcation points: uPVV β −51.097 95% CI [−72.257; −29.937], and crossing points: uPVV $\beta = -48.604$ 95% CI [−74.246; −22.961]), all *P*-values < 0.05. After stratification, the associations were observed in natural conceptions specifically.

LIMITATION, REASONS FOR CAUTION: Although the results of this prospective observational study clearly demonstrate associations between first-trimester utero-placental vascular morphologic development and prenatal growth, further research is required before we can draw firm conclusions about a causal relationship.

WIDER IMPLICATIONS OF THE FINDINGS: Our findings support the hypothesis that morphologic variations in utero-placental vascular development play a role in the vascular mechanisms involved in embryonic and fetal growth and development. Application of the uPVS could benefit our understanding of the pathophysiology underlying placenta-related complications. Future research should focus on the clinical applicability of the uPVS as an imaging marker for the early detection of fetal growth restriction.

STUDY FUNDING/COMPETING INTEREST(S): This research was funded by the Department of Obstetrics and Gynecology of the Erasmus MC, University Medical Centre, Rotterdam, The Netherlands. There are no conflicts of interest.

TRIAL REGISTRATION NUMBER: Registered at the Dutch Trial Register (NTR6854).

Keywords: prenatal growth / placenta / 3D / power Doppler / ultrasound / virtual reality / spiral artery / early pregnancy / vascular morphology / fetal growth restriction

Introduction

Worldwide, impaired prenatal growth, defined as fetal growth restriction (FGR) and infants born small-for-gestational-age (SGA), is an important risk factor for perinatal morbidity and mortality, and has life-course health implications (Lawn *et al.*, 2005; Almond and Currie, 2011; Hanson and Gluckman, 2014; Jaddoe *et al.*, 2014; Malhotra *et al.*, 2019). It is generally recognized that utero-placental vascular development contributes to prenatal growth as it dictates the maternal blood flow to the placenta (Junaid *et al.*, 2014; Burton and Jauniaux, 2018). To provide more insight into vascular mechanisms involved in prenatal growth, it is essential to investigate the first-trimester development of the utero-placental vasculature *in vivo*. The ability to monitor first-trimester utero-placental vascular development in humans will be valuable for the early detection, treatment, and prevention of placenta-related complications.

Ultrasound provides low-cost opportunities for longitudinal non-invasive evaluation of prenatal growth and is widely used in antenatal care. Associations between utero-placental vascular development and prenatal growth have been investigated by a variety of ultrasound markers, including placental volume (PV), vascularization and flow indices, and uterine artery Dopplers (Collins *et al.*, 2013; Reus *et al.*, 2014; Velauthar *et al.*, 2014; Alfirevic *et al.*, 2017; Chen *et al.*, 2022). Evidence suggests utero-placental vascular development and prenatal growth are associated with conception method and fetal sex (Clifton, 2010; Broere-Brown *et al.*, 2016; Rizzo *et al.*, 2016; Cavoretto *et al.*, 2020; Reijnders *et al.*, 2021). Combining three-dimensional (3D) power Doppler (PD) ultrasound and virtual reality (VR), a recent study showed positive associations between utero-placental vascular volume (uPVV) development and embryonic growth, with fetal sex specific modifications (Reijnders *et al.*, 2021). Unfortunately, these studies have not resulted in an imaging marker with potential for early detection of pregnancies at risk for FGR or SGA.

Histopathological research has shown that morphologic variations of the placental vasculature, including vessel caliber and number of remodeled spiral arteries in the placental bed, are associated with prenatal growth (Brosens *et al.*, 2011). However, it is unclear to what extent morphologic variations in the first trimester affect prenatal growth. Recently, our study group has combined 3D PD ultrasound, VR and a skeletonization algorithm to generate the utero-placental vascular skeleton (uPVS) as a structural overview of the utero-placental vascular morphology in the first trimester (de Vos *et al.*, 2022). The uPVS provides information on branching patterns, vascular network length and thickness and can be used to calculate density of vascular branching when combined with uPVV measurements. Using the uPVS, we found decreased utero-placental vascular morphologic development in pregnancies with placenta-related complications (de Vos *et al.*, 2022). Therefore, we hypothesize that uPVS development is

associated with prenatal growth and thus may have potential as an imaging marker for the early detection of FGR and SGA.

In this study, we aim to investigate associations between morphologic development of the utero-placental vasculature and prenatal growth by analyzing associations between uPVS characteristics, density of vascular branching and measurements of embryonic and fetal growth and birth weight. Further, our aim is to investigate whether these associations are affected by conception method, fetal sex and the occurrence of placenta-related complications.

Materials and methods
Ethical approval and study design

The Rotterdam Periconception Cohort (Predict study) was approved by the Institutional Review Board of the Erasmus Medical Centre on 15 October 2004 (MEC-2004-227) (Steegers-Theunissen *et al.*, 2016; Rousian *et al.*, 2021). The VIRTUAL Placenta study, embedded in the Rotterdam Periconception Cohort, was approved by the Institutional Review Board of the Erasmus Medical Centre on 2 June 2015 (MEC 2015-494) (Reijnders *et al.*, 2018).

Women who met the following criteria—a minimum age of 18 years old, a singleton pregnancy with a gestational age (GA) of less than 10 weeks and written informed consent—were recruited from the Erasmus Medical Centre, a tertiary referral hospital in the Netherlands. Both natural conceptions and pregnancies achieved via IVF or ICSI using autologous oocytes were eligible for inclusion.

Study parameters

Between January 2017 and March 2018, participants were enrolled and answered a self-administered questionnaire on general characteristics and medical and obstetric history. At least two study visits were scheduled in the first trimester at 7, 9, and 11 weeks GA, and two study visits at 22 and 32 weeks GA. At the first study visit, height and weight were measured methodically to calculate body-mass index (BMI).

For natural conceptions in regular cycles (25–35 days), GA was calculated from the first day of last menstrual period (LMP). In case of unknown LMP or irregular cycle, GA was calculated from Crown-Rump-Length (CRL). If the two methods varied >6 days, the CRL-based GA was used in pregnancy dating. For fresh IVF-ICSI pregnancies, GA was calculated from oocyte pick-up day +14 days. In case of cryopreserved embryo transfer, GA was calculated from transfer date +19 days.

Pregnancy outcomes were collected through a questionnaire filled out by participants and complemented with medical delivery records. Birth weight was standardized according to Hoftiezer percentiles (Hoftiezer *et al.*, 2016).

Ultrasonography

Trained sonographers performed all ultrasounds using the GE Voluson E8 (GE, Zipf, Austria) with a transvaginal 6–12 MHz transducer. Standardized ultrasound settings were previously described (quality: max; pulse repetition frequency (PRF): 0.6; wall motion filter (WMF): low1; compound resolution imaging (CRI): off; power Doppler (PD) gain: −8.0) (Reijnders *et al.*, 2018).

All first-trimester measurements included transvaginal 3D sweeps of the embryo and gestational sac including the placenta. The utero-placental vasculature was visualized with a 3D PD sweep (Reijnders *et al.*, 2018). All ultrasound examinations were performed according to international guidelines on safe use of Doppler ultrasound in the first trimester of pregnancy (ALARA-principle) (Drukker *et al.*, 2020).

At 22 and 32 weeks GA, transabdominal ultrasonography was performed to measure fetal growth in the second and third trimester, defined as estimated fetal weight (EFW) calculated using the Hadlock formula (Hadlock *et al.*, 1985).

Offline 3D measurements

Image quality was scored as optimal, good, average, or poor based on the presence of artefacts such as blurring of the volume or acoustic shadowing, the ability to distinguish between myometrium and trophoblast, and completeness of the placenta. Images with quality score 'poor' were deemed unusable and excluded from the analyses.

Offline, the V-Scope volume rendering application was used to determine CRL, embryonic volume (EV), and Carnegie stage as measures for embryonic growth and to measure uPVV from the 3D PD sweeps using VR-based segmentation (Supplementary Fig. S1A–C) (Verwoerd-Dikkeboom *et al.*, 2008; O'Rahilly and Muller, 2010; Reijnders *et al.*, 2018; Rousian *et al.*, 2018).

Advanced image processing for retrieving morphologic characteristics

A skeletonization algorithm was applied to the uPVV segmentations to automatically generate the uPVS. This algorithm repeatedly peels off the outermost layer of voxels from the uPVV, reducing the diameter of the PD signal at each point in the vascular network until one central voxel remains, thereby creating a network-like structure representing the vascular morphology (Supplementary Fig. S1D) (de Vos *et al.*, 2022).

Following the construction of the network, the skeletonization algorithm classifies each 26-connected voxel based on the number of neighboring voxels. The algorithm identifies endpoints (one neighbor), bifurcation points (three neighbors), crossing points (four neighbors), and normal vessel points (two neighbors). Voxels with >4 neighbors are considered an artefact and excluded from analyses. Further, the algorithm measures total network length and average vascular thickness (Supplementary Fig. S1E). These six uPVS characteristics represent absolute vascular morphologic development of the first-trimester utero-placental vasculature. Finally, we calculated the number uPVS end-, bifurcation-, and crossing points per cm^3 uPVV to identify three imaging markers to represent the density of vascular branching in the uPVV. A graphic representation of the virtual imaging markers of first-trimester utero-placental vascular development (uPVV, uPVS, and density of vascular branching) is depicted in Fig. 1.

Given the small contribution of embryonic capillaries to the VR-based segmentation and the restricted presence of embryonic flow in the first trimester, we assume the contribution of the embryonic blood space to the uPVV and the uPVS is limited. Therefore, we conclude that the uPVV and uPVS mainly include
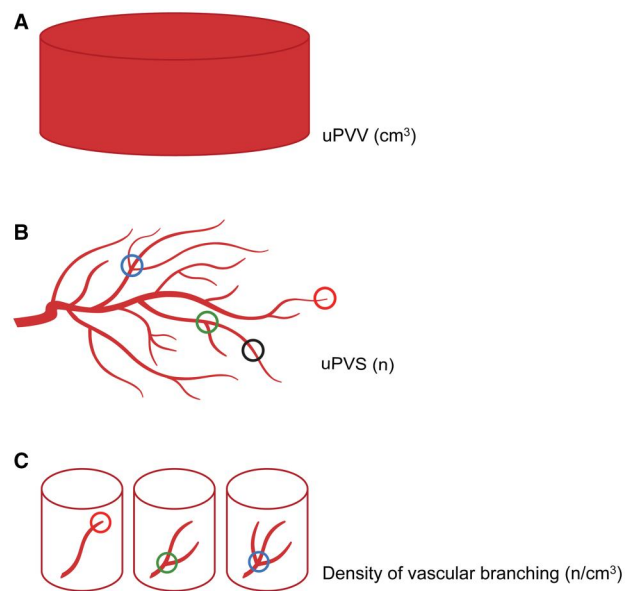
Figure 1. Graphic representation of virtual imaging markers of first-trimester utero-placental vascular development. (**A**) The utero-placental vascular volume (uPVV) measures the total volume of all power Doppler signal within the first-trimester placental tissue up to the placental-myometrial interface in cm^3. (**B**) The utero-placental vascular skeleton (uPVS) measures the number and type of branches within the uPVV. Red circle: voxels that are endpoints. Green circle: voxels that are bifurcation points, Blue circle: voxels that are crossing points. Black circle: voxels that are vessel points (no branch or endpoint). In addition, the total vascular length and average vascular thickness are calculated. (**C**) Density of vascular branching is calculated by dividing the number of endpoints, bifurcation points and crossing points by the uPVV.

the distal segments of the maternal spiral and basal arteries and communicating anastomoses (arteriovenous shunts), see Fig. 2A and B (Reijnders *et al.*, 2018; de Vos *et al.*, 2022).

## Definitions of placenta-related complications

Placenta-related complications were specified as pregnancy-induced hypertension (PIH), preeclampsia (PE), and/or FGR, SGA, or preterm birth (PTB). PIH was defined as new-onset hypertension after 20 weeks GA with systolic blood pressure ≥140 mmHg and/or diastolic blood pressure ≥90 mmHg (Croke, 2019). PE was defined as PIH with the presence of ≥300 mg proteinuria in a 24-h period (Croke, 2019). FGR was defined as a fetal abdominal circumference and/or EFW <10th percentile on the Hadlock curve, or >20 percentile decrease compared to a previous measurement with a minimal timespan of 2 weeks (Gordijn *et al.*, 2016). SGA was defined as birth weight <10th percentile on growth curves specific for GA at birth, parity, and fetal sex (Zeve *et al.*, 2016). PTB was defined as a GA at birth <37 + 0 weeks (Vogel *et al.*, 2018).

Statistical analyses

Baseline characteristics were presented as mean with standard deviation or median with first and third quartiles. If needed, non-volumetric parameters, volumetric parameters, and ratios were transformed using a square root, cubic root and natural log transformation, respectively, to approximate a normal distribution.

Linear mixed models were used to estimate individual trajectories of longitudinal measurements using a quadratic relation with GA. In these models, we allowed for subject-specific intercepts and slopes, the random effects. The models with the best fit included random intercepts only. For Carnegie stages a

First-trimester pregnancy
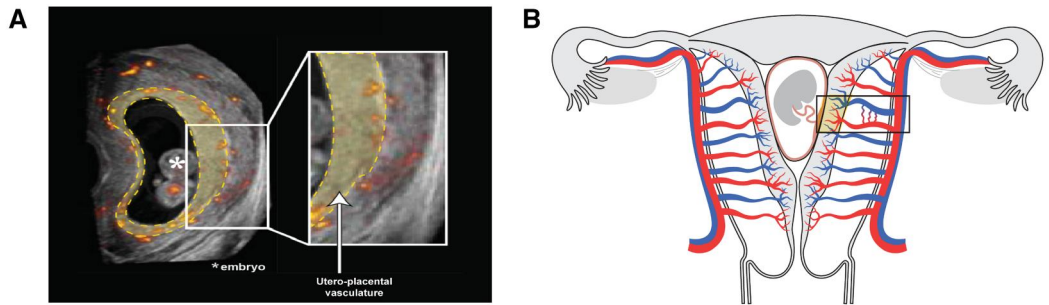
Normal prenatal growth
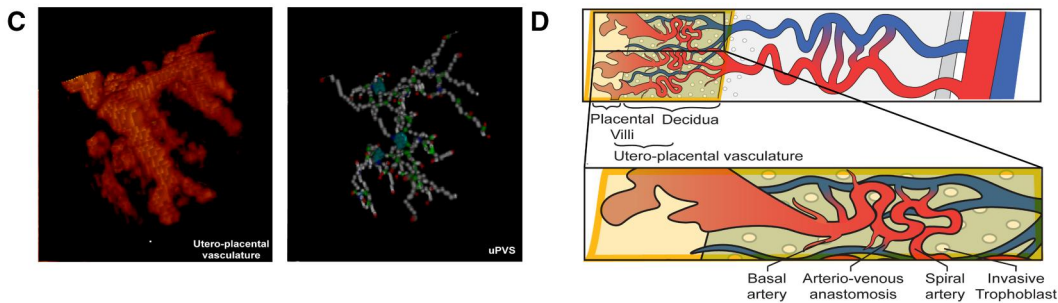
Restricted prenatal growth
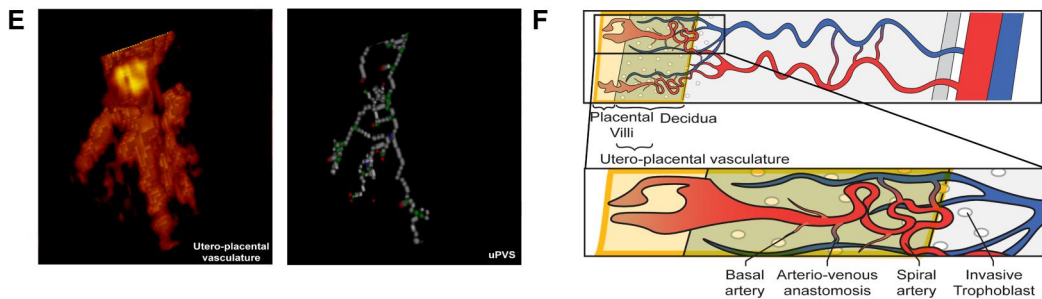
Figure 2. Power Doppler ultrasound and schematic images of the utero-placental vasculature in a first-trimester pregnancy displaying normal and restricted prenatal growth. Overview of the utero-placental vasculature. (**A**) Two-dimensional (2D) power Doppler (PD) ultrasound image of a first-trimester pregnancy; all recorded vasculature is depicted in red-yellow colour. The yellow-highlighted section forms the virtual reality (VR)-based segmentation and corresponds with the yellow box in the schematic images. All vasculature in the VR-based segmentation is included in the utero-placental vascular skeleton (uPVS). (**B**) Schematic image of a first-trimester pregnant uterus including the uterine and placental vasculature (red, arterial vasculature; blue, venous vasculature). The yellow box contains decidua, invasive extravillous trophoblast and placental tissue which form the interface of the utero-placental vasculature. The vascular structures within the utero-placental vasculature are confined to the maternal basal and spiral arteries and their communicating arterio-venous anastomoses, and possibly vessels of the embryonic/foetal-placental blood space. (**C**) Enlarged section of a 3D PD ultrasound image of the utero-placental vasculature and uPVS in pregnancies with normal prenatal growth. The uPVS is characterized by an increased number of end- (red), bifurcation- (green), crossing- (blue), and vessel- (white) points when compared to pregnancies with restricted prenatal growth (as shown in panel E). (**D**) Schematic image of the utero-placental vasculature in pregnancies with normal prenatal growth, characterized by an increased absolute number of branches and arterio-venous anastomosis when compared to pregnancies with restricted prenatal growth. (**E**) Enlarged section of a 3D PD ultrasound image of the utero-placental vasculature and uPVS in pregnancies with restricted prenatal growth. The uPVS is characterized by a decreased number of end- (red), bifurcation- (green), crossing- (blue), and vessel- (white) points when compared to pregnancies with normal prenatal growth. (**F**) Schematic image of the utero-placental vasculature in pregnancies with restricted prenatal growth, characterized by a decreased absolute number of branches and arterio-venous anastomosis when compared to pregnancies with normal prenatal growth.

continuation ratio model with random intercepts was estimated. The random intercepts were used as summaries representing first-trimester utero-placental vascular morphologic development and first-trimester embryonic development.

Hereafter, the summaries of first-trimester utero-placental vascular morphologic development (uPVS characteristics and density of vascular branching) were used as covariates in a linear regression analysis for measures of embryonic growth (summaries of CRL, EV and Carnegie stage development) and fetal growth (EFW at 22 and 32 weeks GA, and birth weight percentiles).

Associations between utero-placental vascular morphologic development and prenatal growth were first assessed in an unadjusted model. A second model was adjusted for maternal age,

BMI, parity, conception mode, smoking, folic acid supplement use and, if appropriate, GA and fetal sex. Potential confounders were selected from literature and discussion amongst authors. In addition, adjusted models were analyzed in subgroups after stratification for conception mode (natural/IVF-ICSI), fetal sex (male/female), and occurrence of placenta-related complications (yes/no).

At last, we applied the Bonferroni correction for multiple testing to reevaluate all our P-values < 0.05 and assessed whether the new level of significance was met.

All analyses were performed using SPSS (version 25.0; SPSS Inc., Chicago, IL, USA) and R (version 4.0.2, R Core Team, Vienna, Austria, 2020). P-values <0.05 were considered statistically significant.

Results
Study population and first-trimester utero-placental vascular morphology
The flowchart of participant selection is depicted in Supplementary Fig. S2. In total, 214 women and 394 respective placental datasets were included in the analysis. Participant characteristics and pregnancy outcomes are depicted in Supplementary Table S1. Supplementary Tables S2 and S3 summarize absolute vascular morphology and density of vascular branching at 7, 9, and 11 weeks GA, respectively.

Utero-placental vascular morphologic development and embryonic growth
Increased absolute vascular morphologic development, estimated by trajectories of the uPVS characteristics, was positively associated with trajectories of CRL (adjusted model: endpoints: $\beta = 0.017$, bifurcation points: $\beta = 0.012$, crossing points: $\beta = 0.017$, vessel points: $\beta = 0.01$, total length: $\beta = 0.007$, all $P \leq 0.01$) and EV (adjusted model: endpoints: $\beta = 0.008$, bifurcation points: $\beta = 0.01$, crossing points: $\beta = 0.008$, vessel points: $\beta = 0.002$, total length: $\beta = 0.003$, all $P \leq 0.01$), see Table 1. Similarly, absolute vascular morphologic development was positively associated with Carnegie stages (endpoints: OR = 1.23, bifurcation points: OR = 1.14, crossing points OR = 1.20, vessel points: OR = 1.06, total length OR = 1.07, all $P < 0.05$), see Table 1.

Next, we stratified for conception mode, fetal sex and the occurrence of placenta-related complications, see Table 2. Absolute vascular morphologic development was positively associated with trajectories of CRL and EV in both natural and IVF-ICSI conceptions, but associations were statistically significant in natural conceptions only. The subgroup analyses for fetal sex showed positive associations for both sexes, but association estimates were higher in females. Further, subgroup analyses showed positive associations with CRL and EV trajectories in both pregnancies with and without placenta-related complications, with higher association estimates in pregnancies with placenta-related complications. All P-values < 0.05. For Carnegie stages, no associations were observed in the subgroup analyses.

Trajectories of density of vascular branching were negatively associated with CRL and EV trajectories, but the associations were not statistically significant and we observed no associations with Carnegie stages, see Supplementary Table S4. After stratification for conception mode, fetal sex, and placenta-related complications, there were no associations between trajectories of the density of vascular branching and trajectories of CRL, EV, or Carnegie stages, see Supplementary Table S5.

After correction for multiple testing using Bonferroni correction, almost all previously significant associations ($P < 0.05$) between uPVS characteristics and CRL and EV remained statistically significant.

Utero-placental vascular morphologic development and fetal growth
Absolute vascular morphologic development, estimated by uPVS trajectories, was positively associated with EFW at 22 weeks GA (adjusted model: uPVS end points: $\beta = 3.379$, bifurcation points: $\beta = 2.134$, crossing points: $\beta = 3.207$, vessel points: $\beta = 0.856$, total length: $\beta = 1.205$, all $P < 0.05$) and EFW at 32 weeks GA (adjusted model: uPVS end points: $\beta = 8.802$, vessel points: $\beta = 2.654$, and total length: $\beta = 3.143$, all $P < 0.05$), see Table 3. We observed no associations between absolute vascular morphologic development and birth weight percentiles.

Again, we stratified for conception mode, fetal sex, and the occurrence of placenta-related complications. Subgroup analyses showed absolute vascular morphologic development was positively associated with EFW at 22 weeks GA and 32 weeks GA in

Table 1. Associations between first-trimester trajectories of absolute utero-placental vascular morphologic development and first-trimester trajectories of embryonic growth and development (n = 214).

Morphologic characteristic	Crown rump length (mm) N = 200 β [95% CI]		Embryonic volume (cm³) N = 192 β [95% CI]		Carnegie stage N = 152 OR [95% CI]	
	Crude	Adjusted	Crude	Adjusted	Crude	Adjusted
$\sqrt{}$uPVS endpoints (n)	0.017 [0.009; 0.025]**	0.017 [0.009; 0.025]**	0.008 [0.004; 0.011]**	0.008 [0.004; 0.012]**	1.244 [1.030; 1.504]*	1.233 [1.013; 1.502]*
$\sqrt{}$uPVS bifurcation points (n)	0.011 [0.006; 0.017]**	0.012 [0.006; 0.018]**	0.005 [0.003 0.008]**	0.005 [0.004; 0.008]**	1.155 [1.017; 1.312]*	1.139 [1.002; 1.295]*
$\sqrt{}$ uPVS crossing points (n)	0.016 [0.009; 0.024]**	0.017 [0.008; 0.025]**	0.007 [0.004 0.011]**	0.008 [0.004; 0.012]**	1.218 [1.022; 1.452]*	1.196 [1.001; 1.429]*
$\sqrt{}$ uPVS vessel points (n)	0.005 [0.002 0.007]**	0.005 [0.002; 0.008]**	0.002 [0.001; 0.003]**	0.002 [0.001; 0.004]**	1.065 [1.008; 1.125]*	1.062 [1.001; 1.126]*
$\sqrt{}$ Total length (mm)	0.006 [0.004; 0.009]**	0.007 [0.004; 0.010]**	0.003 [0.002; 0.004]**	0.003 [0.002; 0.005]**	1.079 [1.013; 1.149]*	1.077 [1.005; 1.154]*
$\sqrt{}$ Average thickness (mm)	−0.270 [−0.614; 0.074]	−0.249 [−0.611; 0.114]	−0.084 [−0.260; 0.093]	−0.084 [−0.267; 0.099]	0.453 [0.000; 369.526]	0.274 [0.000; 596.959]

Depicted are the crude and adjusted estimates: adjusted for maternal age, parity, conception mode, BMI, smoking, preconception initiation of folic acid supplement use, and fetal sex. Carnegie stages (n = 23). uPVS, utero-placental vascular skeleton. Bold text indicates a statistically significant association. Significance at * $P \leq 0.05$, ** $P \leq 0.01$.

Table 2. Associations between first-trimester trajectories of absolute utero-placental vascular morphologic development and first-trimester trajectories of embryonic growth and development, stratified for conception mode, fetal sex, and occurrence of placenta-related complications.

Conception method

	Crown rump length (mm)		Embryonic volume (cm³)		Carnegie stage	
	Adjusted model		Adjusted model		Adjusted model	
	β [95% CI]		β [95% CI]		OR [95% CI]	
Morphologic characteristic	IVF/ICSI (n = 81)	Natural (n = 117)	IVF/ICSI (n = 81)	Natural (n = 112)	IVF/ICSI (n = 77)	Natural (n = 120)
√ uPVS endpoints (n)	0.007 [−0.004; 0.017]	**0.023 [0.010; 0.035]****	0.004 [−0.000; 0.008]	**0.011 [0.004; 0.017]****	1.105 [0.929; 1.316]	1.296 [0.969; 1.733]
√ uPVS bifurcation points (n)	0.004 [−0.003; 0.011]	**0.017 [0.008; 0.026]****	0.003 [−0.001; 0.006]	**0.007 [0.003; 0.012]****	1.076 [0.953, 1.215]	1.197 [0.973, 1.473]
√ uPVS crossing points (n)	0.005 [−0.005; 0.015]	**0.024 [0.012; 0.036]****	0.004 [−0.001; 0.008]	**0.010 [0.004; 0.017]****	1.092 [0.933; 1.278]	1.243 [0.958; 1.613]
√ uPVS vessel points (n)	0.002 [−0.001; 0.005]	**0.007 [0.003; 0.011]****	0.001 [−0.000; 0.003]	**0.003 [0.001; 0.005]****	1.035 [0.979; 1.094]	1.084 [0.989; 1.187]
√ Total length (mm)	0.002 [−0.002; 0.006]	**0.010 [0.006; 0.014]****	0.002 [−0.000; 0.003]	**0.004 [0.002; 0.006]****	1.037 [0.977 1.101]	1.105 [0.992; 1.231]
√ Average thickness (mm)	−0.142 [−0.632; 0.349]	−0.035 [−0.860; 0.167]	−0.046 [−0.259; 0.167]	−0.129 [−0.402; 0.145]	0.045 [0.000; 86.603]	0.269 [0.000; 5038.740]

Fetal sex

	Crown rump length (mm)		Embryonic volume (cm³)		Carnegie stage	
	Adjusted model		Adjusted model		Adjusted model	
	β [95% CI]		β [95% CI]		OR [95% CI]	
Morphologic characteristic	Male (n = 99)	Female (n = 97)	Male (n = 97)	Female (n = 94)	Male (n = 102)	Female (n = 95)
√ uPVS endpoints (n)	0.012 [−0.000; 0.024]	**0.021 [0.009; 0.033]****	**0.007 [0.000; 0.014]***	**0.009 [0.004; 0.014]****	1.108 [0.885; 1.387]	1.452 [0.997; 2.115]
√ uPVS bifurcation points (n)	**0.010 [0.002; 0.018]***	**0.013 [0.004; 0.023]***	**0.005 [0.000; 0.009]***	**0.006 [0.002; 0.010]****	1.071 [0.923; 1.242]	1.342 [0.994; 1.812]
√ uPVS crossing points (n)	**0.014 [0.004; 0.025]****	**0.019 [0.006; 0.032]****	**0.007 [0.001; 0.013]***	**0.008 [0.004; 0.014]****	1.103 [0.896; 1.357]	1.468 [0.965; 2.233]
√ uPVS vessel points (n)	**0.008 [0.001; 0.008]***	**0.006 [0.002; 0.010]****	**0.002 [0.000; 0.004]***	**0.003 [0.001; 0.004]****	1.033 [0.968; 1.103]	1.134 [0.997; 1.290]
√ Total length (mm)	**0.006 [0.002; 0.010]****	**0.008 [0.003; 0.012]****	**0.003 [0.000; 0.005]***	**0.004 [0.002; 0.006]****	1.041 [0.967; 1.121]	1.151 [0.999; 1.327]
√ Average thickness (mm)	−0.078 [−0.543; 0.386]	−0.490 [−1.084; 0.103]	−0.064 [−0.348; 0.221]	0.124 [−0.373; 0.125]	82.980 [0.000; 759573.720]	0.000 [0.000; 17.565]

Placenta-related complications

	Crown rump length (mm)		Embryonic volume (cm³)		Carnegie stage	
	Adjusted model		Adjusted model		Adjusted model	
	β [95% CI]		β [95% CI]		OR [95% CI]	
Morphologic characteristic	With (n = 50)	Without (n = 148)	With (n = 45)	Without (n = 148)	With (n = 51)	Without (n = 146)
√ uPVS endpoints (n)	**0.025 [0.006; 0.045]***	**0.014 [0.005; 0.023]****	0.011 [−0.000; 0.023]	**0.008 [0.004; 0.012]****	1.399 [0.796; 2.458]	1.152 [0.961; 1.380]
√ uPVS bifurcation points (n)	**0.022 [0.007; 0.036]****	**0.009 [0.003; 0.016]****	0.008 [−0.001; 0.017]	**0.005 [0.002; 0.008]****	1.334 [0.865; 2.057]	1.102 [0.956; 1.270]
√ uPVS crossing points (n)	**0.036 [0.015; 0.056]****	**0.013 [0.004; 0.022]****	**0.013 [0.000; 0.027]***	**0.007 [0.003; 0.011]****	1.604 [0.839; 3.067]	1.131 [0.938; 1.364]
√ uPVS vessel points (n)	**0.009 [0.003; 0.015]****	**0.004 [0.001; 0.007]****	0.003 [−0.000; 0.007]	**0.002 [0.001; 0.003]****	1.131 [0.936; 1.366]	1.044 [0.982; 1.110]
√ Total length (mm)	**0.012 [0.005; 0.019]****	**0.006 [0.002; 0.009]****	**0.005 [0.000; 0.009]***	**0.003 [0.002; 0.004]****	1.183 [0.941; 1.487]	1.030 [0.987; 1.076]
√ Average thickness (mm)	−0.501 [−1.375; 0.373]	−0.115 [−0.538; 0.308]	−0.153 [−0.800; 0.494]	−0.030 [−0.219; 0.157]	0.045 [0.000; 8325774.645]	0.38 [0.000; 2481.524]

Depicted are the adjusted estimates: adjusted for maternal age, parity, conception mode, BMI, smoking, folic acid supplement use, and fetal sex. Groups stratified for conception mode were not adjusted for conception mode. Groups stratified for fetal sex were not adjusted for fetal sex. Placenta-related complications are specified as PIH or PE and/or FGR, PTB, and SGA; diagnoses may be overlapping. Carnegie stages (n = 23). uPVS, utero-placental vascular skeleton; PIH, pregnancy-induced hypertension; PE, preeclampsia; FGR, fetal growth restriction; PTB, pre-term birth (including both spontaneous and iatrogenic PTB); SGA, small-for-gestational-age. Bold text indicates a statistically significant association. Significance at * P ≤ 0.05, ** P ≤ 0.01.

Table 3. Associations between first-trimester trajectories of absolute utero-placental vascular morphologic development and second and third trimester of fetal growth, birthweight percentiles.

Morphologic characteristic	Estimated fetal weight second trimester		Estimated fetal weight third trimester		Birth weight percentiles	
	N = 198		N = 193		N = 197	
	β [95% CI]		β [95% CI]		β [95% CI]	
	Crude	Adjusted	Crude	Adjusted	Crude	Adjusted
√ uPVS endpoints (n)	**2.729** [0.398; 5.060]*	**3.379** [0.945; 5.813]**	6.396 [−1.449; 14.241]	**8.802** [0.336; 17.267]*	−0.081 [−1.164; 1.001]	0.020 [−1.159; 1.199]
√ uPVS bifurcation points (n)	**1.677** [0.011; 3.343]*	**2.134** [0.370; 3.897]*	4.012 [−1.628; 9.653]	5.697 [−0.438; 11.831]	0.223 [−0.573; 1.019]	0.293 [−0.569; 1.155]
√ uPVS crossing points (n)	**2.608** [0.295; 4.921]*	**3.207** [0.744; 5.670]*	5.499 [−2.384; 13.381]	7.454 [−1.155; 16.063]	0.421 [−0.696; 1.537]	0.502 [−0.713; 1.717]
√ uPVS vessel points (n)	0.666 [−0.055; 1.388]	**0.856** [0.094; 1.618]*	1.879 [−0.556; 4.314]	**2.654** [0.019; 5.290]*	0.091 [−0.251; 0.434]	0.124 [−0.246; 0.494]
√ Total length (mm)	**0.977** [0.144; 1.810]*	**1.205** [0.317; 2.092]**	2.398 [−0.434; 5.230]	**3.143** [0.044; 6.243]*	0.025 [−0.028; 0.078]	0.026 [−0.024; 0.0767]
√ Average thickness (mm)	−39.248 [−141.346; 62.850]	−57.724 [−163.541; 48.093]	−35.841 [−377.592; 305.886]	−81.313 [−446.481; 284.329]	16.363 [−30.929; 63.655]	14.874 [−34.744; 64.4934]

Depicted are the crude and adjusted estimates: adjusted for maternal age, parity, conception mode, BMI, smoking, and preconception initiation of folic acid supplement use. Models for estimated fetal weight (EFW) in the second and third trimesters are additionally adjusted for gestational age and fetal sex. Second-trimester EFW was measured at 22 weeks gestational age (GA) and third-trimester EFW was measured at 32 weeks GA. uPVS, utero-placental vascular skeleton; GA, gestational age. Bold text indicates a statistically significant association. Significance at   * $P \leq 0.05$,   ** $P \leq 0.01$.

natural conceptions and pregnancies with placenta-related complications only, see Table 4.

Finally, we found negative associations between trajectories of density of vascular branching and EFW at 32 weeks GA (adjusted model: density of endpoints: $\beta = -94.972$, density of bifurcation points: $\beta = -192.601$, all $P < 0.05$) and birth weight percentiles (adjusted model: density of endpoints: $\beta = -20.727$, density of bifurcation points: $\beta = -51.097$, density of crossing points: $\beta = -48.604$, all $P < 0.05$), see Table 5.

After stratification for conception mode, fetal sex, and the occurrence of placenta-related complications, trajectories of density of vascular branching are negatively associated with EFW at 32 weeks GA and birth weight percentiles in natural conceptions only. Further, subgroup analyses showed negative associations between trajectories of density of vascular branching and birth weight percentiles for both males and females, with higher association estimates in females. Finally, density of vascular branching was negatively associated with EFW in the second and third trimester and birth weight percentiles in pregnancies with placenta-related complications. In pregnancies without placenta-related complications negatively associations were observed with birth weight percentiles only, see Table 6.

After correction for multiple testing using Bonferroni correction, almost all previously significant associations ($P < 0.05$) between density characteristics and birth weight percentiles remained statistically significant.

Discussion
Principal findings
This study demonstrates associations between absolute vascular morphologic development and density of vascular branching and embryonic and fetal growth using the uPVS as a new imaging marker of first-trimester utero-placental vascular morphologic development. Our findings suggest increased development of absolute vascular morphologic development is favorable for prenatal growth, specifically in natural conceptions and pregnancies with placenta-related complications. Furthermore, negative

associations between first-trimester density of vascular branching and embryonic and fetal growth suggest aberrant vascular development negatively affects prenatal growth, with effects notable in birth weight percentiles. All associations are stronger in pregnancies of a female fetus. Fig. 2C–F provides a graphic summary of our interpretation of this study's findings.

Results in the context of what is known
An important foundation for prenatal growth is established in the periconception period, defined as 14 weeks prior up to 10 weeks after conception (Steegers-Theunissen et al., 2013). During this period, the development of the utero-placental vasculature is mediated by trophoblast invasion, which disrupts spiral artery walls and forms intraluminal plugs that prevent maternal blood flow toward the placenta and developing embryo (Kaufmann et al., 2003; Weiss et al., 2016). The resultant physiological low-oxygen environment promotes angiogenesis which is essential to secure adequate early development of the utero-placental vasculature and safeguards the biological growth potential (Sun et al., 2020).

In cases where trophoblast invasion is defective, remodeling of the spiral arteries is inadequate and trophoblast plugs disintegrate prematurely (Jauniaux et al., 2003; Burton et al., 2009; James et al., 2018; Saghian et al., 2019). Untimely influx of maternal blood flow at high velocity induces oxidative stress and tissue damage to the placental bed, which in the worst case results in miscarriage (Jauniaux et al., 2000, 2003; Burton et al., 2009). In less severe cases, the placental damage results in impaired placental function and can ultimately cause PE and FGR (Burton and Jauniaux, 2004, 2018; Huppertz, 2018; Schoots et al., 2018). We believe the absolute vascular morphologic development reflects spiral artery remodeling and the subsequent (mal-)development of the utero-placental vasculature and is therefore associated with prenatal growth. Furthermore, we postulate an increased density of vascular branching reflects a, conceivably compensatory, abnormal vascular development that follows aberrant spiral artery remodeling, and is accordingly associated with

Table 4. Associations between first-trimester trajectories of absolute utero-placental vascular morphologic development and second and third trimester of fetal growth, birthweight percentiles after stratification for conception method, fetal sex, and occurrence of placenta-related complications.

	Estimated fetal weight second trimester		Estimated fetal weight third trimester		Birth weight percentiles	
	Adjusted model		Adjusted model		Adjusted model	
Conception method	β [95% CI]		β [95% CI]		β [95% CI]	
Morphologic characteristic	IVF/ICSI (n = 81)	Natural (n = 117)	IVF/ICSI (n = 81)	Natural (n = 112)	IVF/ICSI (n = 77)	Natural (n = 120)
√ uPVS endpoints (n)	−2.490 [−1.652; 6.631]	**4.655 [2.157; 7.152]****	11.090 [−3.506; 25.686]	7.139 [−3.319; 17.578]	0.794 [−0.891; 2.478]	−0.733 [−2.433; 0.967]
√ uPVS bifurcation points (n)	0.736 [−2.265 3.736]	**3.591 [1.840; 5.342]****	5.834 [−4.820; 16.489]	**7.711 [0.287; 15.135]***	0.522 [−0.738; 1.783]	0.087 [−1.140; 1.313]
√ uPVS crossing points (n)	1.230 [−2.992; 5.451]	**4.938 [2.491; 7.385]****	6.840 [−8.314; 21.995]	**11.031 −0.698; 21.363]***	0.714 [−1.067; 2.496]	0.278 [−1.460; 2.016]
√ uPVS vessel points (n)	0.280 [−1.029; 1.589]	**1.505 [0.751; 2.259]***	2.8501 [−1.764; 7.464]	**3.336 [0.156; 6.517]***	0.263 [−0.282; 0.808]	0.006 [−0.518; 0.530]
√ Total length (mm)	0.395 [−1.098; 1.888]	**1.997 [1.112; 2.882]****	2.681 [−2.631; 7.992]	**4.536 [0.738; 8.335]***	0.238 [−0.391; 0.866]	0.202 [−0.424; 0.833]
√ Average thickness (mm)	−26.855 [−232.422; 178.713]	−70.086 [−172.889; 32.716]	−249.171 [−987.203; 488.861]	−124.407 [−534.432; 285.618]	−42.889 [−129.345; 43.566]	41.509 [−22.021; 105.038]

	Estimated fetal weight second trimester		Estimated fetal weight third trimester		Birth weight percentiles	
	Adjusted model		Adjusted model		Adjusted model	
Fetal sex	β [95% CI]		β [95% CI]		β [95% CI]	
Morphologic characteristic	Male (n = 99)	Female (n = 97)	Male (n = 97)	Female (n = 94)	Male (n = 102)	Female (n = 95)
√ uPVS endpoints (n)	2.676 [−0.147; 5.499]	**4.258 [0.710; 7.806]***	**13.400 [0.705; 26.095]***	4.758 [v6.492; 16.007]	0.765 [−1.003; 2.533]	−0.769 [−2.457; 0.920]
√ uPVS bifurcation points (n)	1.794 [−0.184; 3.772]	1.994 [−0.676; 4.663]	6.879 [−2.072; 15.830]	6.155 [−2.112; 14.423]	0.260 [−0.983; 1.503]	0.331 [−0.944; 1.605]
√ uPVS crossing points (n)	2.349 [−0.368; 5.066]	3.375 [−0.420; 7.171]	6.959 [−5.477; 19.395]	11.257 [−0.451; 22.966]	0.243 [−1.467; 1.951]	0.798 [−1.042; 2.638]
√ uPVS vessel points (n)	0.763 [−0.092; 1.617]	1.792 [−0.363; 1.947]	3.204 [−0.649; 7.056]	2.713 [−0.854; 6.280]	0.119 [−0.417; 0.655]	0.135 [−0.413; 0.683]
√ Total length (mm)	**1.024 [0.487; 2.000]***	1.111 [−0.260; 2.482]	3.677 [−0.758; 8.111]	3.215 [−1.043; 7.473]	0.258 [−0.358; 0.874]	0.193 [−0.461; 0.847]
√ Average thickness (mm)	−45.271 [−158.894; 68.352]	−33.734 [−206.222; 138.755]	−235.663 [−747.501; 276.175]	−93.207 [633.538; 447.124]	10.583 [−59.245; 80.411]	18.265 [−59.741; 96.271]l

	Estimated fetal weight second trimester		Estimated fetal weight third trimester		Birth weight percentiles	
	Adjusted model		Adjusted model		Adjusted model	
Placenta-related complications	β [95% CI]		β [95% CI]		β [95% CI]	
Morphologic characteristic	With (n = 50)	Without (n = 148)	With (n = 45)	Without (n = 148)	With (n = 51)	Without (n = 146)
√ uPVS endpoints (n)	4.259 [−0.900; 9.418]	1.967 [−0.718; 4.652]	16.548 [−5.147; 38.244]	6.035 [−2.178; 14.247]	−0.209 [−2.830; 2.412]	0.020 [−1.183; 1.224]
√ uPVS bifurcation points (n)	**4.465 [0.810; 8.121]***	0.992 [−0.939; 2.923]	**21.757 [6.853; 36.661]****	0.946 [−4.999; 6.891]	0.735 [−1.190; 2.660]	−0.071 [−0.944; 0.802]
√ uPVS crossing points (n)	**6.993 [1.491; 12.496]***	1.663 [−0.986; 4.312]	**27.395 [3.117; 51.674]***	1.099 [−7.061; 9.258]	0.743 [−2.196; 3.683]	0.047 [−1.162; 1.256]
√ uPVS vessel points (n)	**1.852 [0.271; 0.432]***	0.375 [−0.458; 1.207]	**9.414 [2.984; 15.844]****	0.586 [−1.972; 3.144]	0.348 [−0.479; 1.174]	−0.039 [−0.413; 0.336]
√ Total length (mm)	**2.539 [0.748; 4.331]****	0.582 [−0.395; 1.558]	**10.824 [3.123; 18.525]****	0.764 [−2.241; 3.769]	0.339 [−0.641; 1.319]	0.051 [−0.390; 0.492]
√ Average thickness (mm)	−90.068 [−295.575; 115.439]	−8.738 [−131.113; 113.637]	−515.893 [−1382.235; −350.449]	154.427 [−219.395; 528.249]	−20.486 [−120.205; 79.233]	33.857 [−19.316; 87.030]

Depicted are adjusted estimates: adjusted for maternal age, parity, conception mode, BMI, smoking, and folic acid supplement use. Models for Estimated fetal weight (EFW) in the second and third trimesters are additionally adjusted for gestational age and fetal sex. Groups stratified for conception mode were not adjusted for conception mode. Groups stratified for fetal sex were not adjusted for fetal sex. Second trimester EFW was measured at 22 weeks gestational age (GA) and third trimester EFW was measured at 32 weeks GA. Placenta-related complications are specified as PIH or PE and/or FGR, PTB. uPVS, utero-placental vascular skeleton; GA, gestational age; PIH, pregnancy-induced hypertension; PE, preeclampsia; FGR, fetal growth restriction; PTB, pre-term birth (including both spontaneous and iatrogenic PTB); SGA, small-for-gestational-age. Bold text indicates a statistically significant association. Significance at * P ≤ 0.05, ** P ≤ 0.01.

Table 5. Associations between first-trimester trajectories of density of vascular branching (number of uPVS points per cm^3 uPVV) and second and third trimesters of fetal growth and birthweight percentiles.

Morphologic characteristic	Estimated fetal weight second trimester		Estimated fetal weight third trimester		Birth weight percentiles	
	N = 198		N = 193		N = 197	
	β [95% CI]		β [95% CI]		β [95% CI]	
	Crude	Adjusted	Crude	Adjusted	Crude	Adjusted
ln Density of endpoints (n/cm^3)	−10.053 [−35.679; 15.574]	−12.906 [−39.164; 13.351]	**−91.573 [−178.096; −5.050]***	**−94.972 [−185.245; −3.698]***	**−20.516 [−31.972 −9.060]****	**−20.727 [−32.771; −8.683]****
ln Density of bifurcation points (n/cm^3)	−8.957 [−56.085; 38.172]	−10.654 [−59.676; 38.368]	**−197.255 [−354.597]***	**−192.601 [−360.532; −24.670]***	**−49.892 [−70.122; −29.663]****	**−51.097 [−72.257; −29.937]****
ln Density of crossing points (n/cm^3)	28.464 [−25.889; 82.818]	32.211 [−24.756; 89.167]	**−175.821 [−351.500; −0.142]***	−179.422 [−367.676; 8.832]	**−47.356 [−71.725; −22.988]****	**−48.604 [−74.246; −22.961]****

Depicted are adjusted estimates: adjusted for maternal age, parity, conception mode, BMI, smoking, and folic acid supplement use. Models for estimated fetal weight (EFW) in the second and third trimesters are additionally adjusted for gestational age and fetal sex. Second-trimester EFW was measured at 22 weeks gestational age (GA) and third-trimester EFW was measured at 32 weeks GA. uPVS, utero-placental vascular skeleton; uPVV, utero-placental vascular volume; GA, gestational age. Bold text indicates a statistically significant association. Significance at * $P \leq 0.05$, ** $P \leq 0.01$.

impaired prenatal growth (Borowicz and Reynolds, 2010; Coan et al., 2010; Stenhouse et al., 2019; Huang et al., 2021).

Interestingly, significant associations between uPVS imaging markers and prenatal growth are observed more frequently in natural conceptions than in IVF-ICSI pregnancies. Contrary to our observations, previous studies have shown IVF to be associated with aberrant placental development and consequently an increased risk of FGR (Zhao et al., 2020; Kong et al., 2022). The aberrant placental development in IVF seems predominantly mediated by the hormonal environment and the subsequent epigenetic changes that are the result of ovarian stimulation (Senapati et al., 2018). Another explanation for why we observed no associations in the IVF-ICSI subgroup, may be the fact that there were fewer pregnancies with a placenta-related complication and significantly fewer cases of SGA in this subgroup (3.4% in the IVF-ICSI group vs 12.6% in natural group). We performed an additional analysis in which all pregnancies with a placenta-related complication were excluded. This sensitivity analysis showed similar results to the stratified analysis of the total cohort (data not shown).

Sex differences between males and females contribute to altered prenatal growth and fetal outcomes. While males tend to prioritize physical growth, which ensures a higher birth weight and superior length into adulthood, females tend to invest in placental reserve, making them less vulnerable to placenta-related complications (Eriksson et al., 2010; Meakin et al., 2021). These sex-dependent differences are in accordance with our observations that utero-placental vascular morphologic development seems to be more strongly associated with fetal growth in females.

Using the uPVS, we previously observed decreased absolute vascular morphologic development in pregnancies with placenta-related complications compared to pregnancies without these complications (de Vos et al., 2022). Interestingly, the present study shows embryonic and fetal growth is more positively associated with morphologic development of the utero-placental vasculature in pregnancies with placenta-related complications. These results are in line with our hypothesis and imply that morphologic development of the first-trimester utero-placental vasculature seems to play a more important, perhaps compensatory, role in regulating prenatal growth in pregnancies with placenta-related complications.

Clinical implications

This prospective observational study suggests that morphologic variations in the utero-placental vascular development play a role in vascular mechanisms involved in embryonic and fetal growth. The clinical applicability of the uPVS as an early imaging marker for detection of FGR and SGA needs further investigation.

Research implications

This study was conducted in a tertiary referral hospital population. Correspondingly, the study population mainly consists of high-risk pregnancies, and over 40% are conceived via IVF-ICSI treatment. Extrapolation of this study's findings to the general population needs to be exercised with consideration. We advise to validate the uPVS in a large population-based cohort.

Strengths and limitations

To our knowledge, this is the first study to investigate associations between in vivo morphologic development of first-trimester human utero-placental vasculature and prenatal growth. This study's main strengths are the serial collection of 3D PD ultrasound data in the early first trimester and the use of validated uPVV segmentations (ICC above 0.80 and relative differences of less than 20%) for automated generation of the uPVS (Reijnders et al., 2018). Further, we applied advanced statistical models for adjustment of maternal age, parity, conception mode, BMI, smoking, alcohol consumption, and folic acid supplement use.

According to our study protocol, we used standardized PD gain settings for all participants. As a result, we cannot account for the possible variability, specifically noted for transabdominal ultrasound acquisition, in power Doppler display given the interperson variability in acoustic properties and placental position, which might have affected variations in the uPVS. However, we believe this issue is mitigated by the use of the transvaginal approach which bypasses the abdominal wall and reduces the distance to the area of interest.

As a result of the observational character of this study, we cannot draw conclusions about causality between first-trimester utero-placental vascular morphologic development and prenatal

Table 6. Associations between first-trimester trajectories of density of vascular branching (number of uPVS points per cm³ uPVV) and second and third trimester of fetal growth, birthweight percentiles after stratification for conception method, fetal sex, and occurrence of placenta-related complications.

Conception method

Morphologic characteristic	Estimated fetal weight second trimester		Estimated fetal weight third trimester		Birth weight percentiles	
	Adjusted model β [95% CI]		Adjusted model β [95% CI]		Adjusted model β [95% CI]	
	IVF/ICSI (n = 81)	Natural (n = 117)	IVF/ICSI (n = 81)	Natural (n = 112)	IVF/ICSI (n = 77)	Natural (n = 120)
ln Density of endpoints (n/cm³)	27.174 [−23.516; 77.864]	**−27.897 [−53.137; −2.658]***	−48.744 [−231.258; 133.769]	**−150.942 [−251.109; −50.776]****	−10.793 [−32.495; 10.910]	**−25.548 [−40.676; −10.420]****
ln Density of bifurcation points (n/cm³)	50.927 [−48.784; 150.641]	−20.889 [−67.410; 15.631]	−95.358 [−455.878; 265.162]	**−237.017 [−418.023; −56.012]***	−20.691 [−62.410; 21.038]	**−62.802 [−88.457; −37.147]****
ln Density of crossing points (n/cm³)	85.339 [−23.151; 193.830]	9.319 [−46.081; 64.720]	−110.353; [−485.160; 264.454]	−183.700 [−397.124; 29.723]	−7.327 [−53.671; 39.017]	**−68.725 [−100.127; −37.202]****

Fetal sex

Morphologic characteristics	Estimated fetal weight second trimester		Estimated fetal weight third trimester		Birth weight percentiles	
	Adjusted model β [95% CI]		Adjusted model β [95% CI]		Adjusted model β [95% CI]	
	Male (n = 99)	Female (n = 97)	Male (n = 97)	Female (n = 94)	Male (n = 102)	Female (n = 95)
ln Density of endpoints (n/cm³)	**−29.912 [−57.883; −1.942]***	27.572 [−13.833; 68.978]	−93.075 [−221.651; 35.501]	−114.636 [−241.440; 12.167]	**−17.566 [−35.086; −0.046]***	**−27.255 [−45.234; −9.277]****
ln Density of bifurcation points (n/cm³)	−47.632 [−101.794; 7.070]	46.894 [−26.928; 120.716]	−146.456 [−400.012; 107.100]	−202.562 [−429.245; 24.120]	**−48.497 [−81.087; −15.908]****	**−57.449 [−88.156; −26.742]****
ln Density of crossing points (n/cm³)	−34.756 [−99.947; 30.434]	**98.098 [15.207; 180.989]***	−208.955 [−498.120; 80.209]	−59.381 [−325.765; 207.003]	**−52.002 [−90.449; −13.554]****	**−52.682 [−90.611; −14.754]****

Placenta-related complications

Morphologic characteristics	Estimated fetal weight second trimester		Estimated fetal weight third trimester		Birth weight percentiles	
	Adjusted model β [95% CI]		Adjusted model β [95% CI]		Adjusted model β [95% CI]	
	With (n = 50)	Without (n = 148)	With (n = 45)	Without (n = 148)	With (n = 51)	Without (n = 146)
ln Density of endpoints (n/cm³)	**−63.850 [−107.370; −20.330]****	10.410 [−20.276; 41.089]	**−379.193 [−557.827; −200.559]****	37.537 [−56.359; 131.433]	**−35.546 [−57.913; −13.178]****	−6.918 [−20.330; 6.494]
ln Density of bifurcation points (n/cm³)	**−102.500 [−185.935; −19.110]***	26.531 [−30.824; 83.885]	**−455.436 [−820.730; −90.142]***	3.097 [−173.380; 179.575]	**−63.431 [−104.819; −22.042]****	**−31.574 [−55.689; −7.458]****
ln Density of crossing points (n/cm³)	−82.951 [−196.213; 30.311]	55.154 [−8.231; 118.538]	−327.953 [−808.706; 152.800]	−21.290 [−206.993; 164.413]	**−63.556 [−114.917; −12.195]***	**−28.352 [−56.111; −0.592]***

Depicted are adjusted estimates: adjusted for gestational age and fetal sex. Groups stratified for conception mode were not adjusted for conception mode. Models for estimated fetal weight (EFW) in the second and third trimester are additionally adjusted for maternal age, parity, conception mode, BMI, smoking, and folic acid supplement use. Models stratified for fetal sex were not adjusted for fetal sex. Second trimester EFW was measured at 22 weeks gestational age (GA) and third trimester EFW was measured at 32 weeks GA. Placenta-related complications are specified as PIH or PE and/or FGR, PTB and SGA; diagnoses may be overlapping. uPVS, utero-placental vascular skeleton; GA, gestational age; PIH, pregnancy-induced hypertension; PE, preeclampsia; FGR, fetal growth restriction; PTB, pre-term birth (including both spontaneous and iatrogenic PTB); SGA, small-for-gestational-age. Bold text indicates a statistically significant association. Significance at * $P \leq 0.05$, ** $P \leq 0.01$.

growth. Also, as stratification impacts group size, the results of our subgroup analysis need to be interpreted with consideration. The group of placenta-related complications was highly heterogeneous. We were not able to distinguish between spontaneous and iatrogenic PTB. Because of the size of the study population, we could not analyze SGA, which consists of constitutionally small infants, and FGR, which includes infants that fail to reach their biological growth potential, separately (Audette and Kingdom, 2018). However, we argue that exclusive stratification for FGR-fetuses would likely increase the strength of the associations between vascular morphologic development and prenatal growth.

We performed multiple statistical analyses, mainly to substantiate whether all imaging markers of utero-placental vascular development are associated with embryonic and fetal growth and birth weight percentiles. Previously, uPVV and uPVS characteristics were highly correlated and are inversely correlated with the density of vascular branching (de Vos et al., 2022). Therefore, the positive correlations between the effect estimates of uPVV and uPVS characteristics and the inverse correlation with density of vascular branching found in the present study can be interpreted as internal validation and we assume that multiple testing is not a significant issue in our study.

Conclusions

The uPVS, a novel imaging marker of utero-placental vascular morphology, is associated with embryonic and fetal growth. Positive associations between first-trimester uPVS characteristics and prenatal growth suggest increased absolute vascular morphologic development is favorable for prenatal growth. Furthermore, increased density of vascular branching, apparently reflecting aberrant vascular development, is associated with decreased prenatal growth. Our findings suggest morphologic variations in the utero-placental vascular development play a role in the vascular mechanisms involved in embryonic and fetal growth. Further, these associations seem to be affected by conception method, fetal sex and the occurrence of placenta-related complications. The clinical applicability of the uPVS as an imaging marker for early detection of FGR and SGA requires further investigation.

Supplementary data

Supplementary data are available at *Human Reproduction* online.

Data availability

The data underlying this article will be shared on reasonable request to the corresponding author.

Acknowledgements

Authors' roles

Funding

Conflict of interest

None declared.

References

Alfirevic Z, Stampalija T, Dowswell T. Fetal and umbilical Doppler ultrasound in high-risk pregnancies. *Cochrane Database Syst Rev* 2017;**6**:CD007529.

Almond D, Currie J. Killing me softly: the fetal origins hypothesis. *J Econ Perspect* 2011;**25**:153–172.

Audette MC, Kingdom JC. Screening for fetal growth restriction and placental insufficiency. *Semin Fetal Neonatal Med* 2018;**23**:119–125.

Borowicz P, Reynolds LP. 'Placental programming': more may still be less. *J Physiol* 2010;**588**:393–393.

Broere-Brown ZA, Schalekamp-Timmermans S, Hofman A, Jaddoe VWV, Steegers EAP. Fetal sex dependency of maternal vascular adaptation to pregnancy: a prospective population-based cohort study. *BJOG* 2016;**123**:1087–1095.

Brosens I, Pijnenborg R, Vercruysse L, Romero R. the "great obstetrical syndromes" are associated with disorders of deep placentation. *Am J Obstet Gynecol* 2011;**204**:193–201.

Burton GJ, Jauniaux E. Placental oxidative stress: from miscarriage to preeclampsia. *J Soc Gynecol Investig* 2004;**11**:342–352.

Burton GJ, Jauniaux E. Pathophysiology of placental-derived fetal growth restriction. *Am J Obstet Gynecol* 2018;**218**:S745–S761.

Burton GJ, Woods AW, Jauniaux E, Kingdom JC. Rheological and physiological consequences of conversion of the maternal spiral arteries for uteroplacental blood flow during human pregnancy. *Placenta* 2009;**30**:473–482.

Cavoretto PI, Farina A, Miglio R, Zamagni G, Girardelli S, Vanni VS, Morano D, Spinillo S, Sartor F, Candiani M. Prospective longitudinal cohort study of uterine arteries Doppler in singleton pregnancies obtained by IVF/ICSI with oocyte donation or natural conception. *Hum Reprod* 2020;**35**:2428–2438.

Chen JY, Chen M, Wu XJ, Sun JM, Zhang Y, Li YF, Zhong LY, Yu BL, Luo J, Liu JH. The value of placental vascularization indices for predicting preeclampsia and fetal growth restriction in different stages of gestation: a prospective and longitudinal study. *Placenta* 2022;**122**:1–8.

Clifton VL. Review: sex and the human placenta: mediating differential strategies of fetal growth and survival. *Placenta* 2010; **31**:S33–S39.

Coan PM, Vaughan OR, Sekita Y, Finn SL, Burton GJ, Constancia M, Fowden AL. Adaptations in placental phenotype support fetal growth during undernutrition of pregnant mice. *J Physiol* 2010; **588**:527–538.

Collins SL, Stevenson GN, Noble JA, Impey L. Rapid calculation of standardized placental volume at 11 to 13 weeks and the

prediction of small for gestational age babies. *Ultrasound Med Biol* 2013;**39**:253–260.

Croke L. Gestational hypertension and preeclampsia: a practice bulletin from ACOG. *Am Family Phys* 2019;**100**:649–650.

de Vos ES, Koning AHJ, Steegers-Theunissen RPM, Willemsen SP, van Rijn BB, Steegers EAP, Mulders A. Assessment of first-trimester utero-placental vascular morphology by 3D power Doppler ultrasound image analysis using a skeletonization algorithm: the Rotterdam Periconception Cohort. *Hum Reprod* 2022;**37**:2532–2545.

Drukker L, Droste R, Chatelain P, Noble JA, Papageorghiou AT. (2020). Safety indices of ultrasound: adherence to recommendations and awareness during routine obstetric ultrasound scanning. *Ultraschall Med* **41**:138–145.

Eriksson JG, Kajantie E, Osmond C, Thornburg K, Barker DJP. Boys live dangerously in the womb. *Am J Hum Biol* 2010;**22**:330–335.

Gordijn SJ, Beune IM, Thilaganathan B, Papageorghiou A, Baschat AA, Baker PN, Silver RM, Wynia K, Ganzevoort W. Consensus definition of fetal growth restriction: a Delphi procedure. *Ultrasound Obstet Gynecol* 2016;**48**:333–339.

Hadlock FP, Harrist RB, Sharman RS, Deter RL, Park SK. Estimation of fetal weight with the use of head, body, and femur measurements—a prospective study. *Am J Obstet Gynecol* 1985;**151**:333–337.

Hanson MA, Gluckman PD. Early developmental conditioning of later health and disease: physiology or pathophysiology? *Physiol Rev* 2014;**94**:1027–1076.

Hoftiezer L, Hukkelhoven CW, Hogeveen M, Straatman HM, van Lingen RA. Defining small-for-gestational-age: prescriptive versus descriptive birthweight standards. *Eur J Pediatr* 2016;**175**:1047–1057.

Huang Z, Huang S, Song T, Yin Y, Tan C. Placental angiogenesis in mammals: a review of the regulatory effects of signaling pathways and functional nutrients. *Adv Nutr* 2021;**12**:2415–2434.

Huppertz B. The critical role of abnormal trophoblast development in the etiology of preeclampsia. *Curr Pharm Biotechnol* 2018;**19**:771–780.

Jaddoe VW, de Jonge LL, Hofman A, Franco OH, Steegers EA, Gaillard R. First trimester fetal growth restriction and cardiovascular risk factors in school age children: population based cohort study. *BMJ* 2014;**348**:g14.

James JL, Saghian R, Perwick R, Clark AR. Trophoblast plugs: impact on utero-placental haemodynamics and spiral artery remodelling. *Hum Reprod* 2018;**33**:1430–1441.

Jauniaux E, Hempstock J, Greenwold N, Burton GJ. Trophoblastic oxidative stress in relation to temporal and regional differences in maternal placental blood flow in normal and abnormal early pregnancies. *Am J Pathol* 2003;**162**:115–125.

Jauniaux E, Watson AL, Hempstock J, Bao YP, Skepper JN, Burton GJ. Onset of maternal arterial blood flow and placental oxidative stress—a possible factor in human early pregnancy failure. *Am J Pathol* 2000;**157**:2111–2122.

Junaid TO, Brownbill P, Chalmers N, Johnstone ED, Aplin JD. Fetoplacental vascular alterations associated with fetal growth restriction. *Placenta* 2014;**35**:808–815.

Kaufmann P, Black S, Huppertz B. Endovascular trophoblast invasion: implications for the pathogenesis of intrauterine growth retardation and preeclampsia. *Biol Reprod* 2003;**69**:1–7.

Kong F, Fu Y, Shi H, Li R, Zhao Y, Wang Y, Qiao J. Placental abnormalities and placenta-related complications following *in-vitro* fertilization: based on national hospitalized data in China. *Front Endocrinol (Lausanne)* 2022;**13**:924070.

Lawn JE, Cousens S, Zupan J. Lancet neonatal survival steering T. 4 million neonatal deaths: when? Where? Why? *Lancet* 2005;**365**:891–900.

Malhotra A, Allison BJ, Castillo-Melendez M, Jenkin G, Polglase GR, Miller SL. Neonatal morbidities of fetal growth restriction: pathophysiology and impact. *Front Endocrinol (Lausanne)* 2019;**10**:55.

Meakin AS, Cuffe JSM, Darby JRT, Morrison JL, Clifton VL. Let's talk about placental sex, baby: understanding mechanisms that drive female- and male-specific fetal growth and developmental outcomes. *IJMS* 2021;**22**:6386.

O'Rahilly R, Muller F. Developmental stages in human embryos: revised and new measurements. *Cells Tissues Organs* 2010;**192**:73–84.

Reijnders IF, Mulders A, Koster MPH, Koning AHJ, Frudiger A, Willemsen SP, Jauniaux E, Burton GJ, Steegers-Theunissen RPM, Steegers EAP. New imaging markers for preconceptional and first-trimester utero-placental vascularization. *Placenta* 2018;**61**:96–102.

Reijnders IF, Mulders A, Koster MPH, Kropman ATM, de Vos ES, Koning AHJ, Willemsen SP, Rousian M, Steegers EAP, Steegers-Theunissen RPM. First-trimester utero-placental (vascular) development and embryonic and fetal growth: the Rotterdam Periconception Cohort. *Placenta* 2021;**108**:81–90.

Reus AD, Klop-van der Aa J, Rifouna MS, Koning AH, Exalto N, van der Spek PJ, Steegers EA. Early pregnancy placental bed and fetal vascular volume measurements using 3-D virtual reality. *Ultrasound Med Biol* 2014;**40**:1796–1803.

Rizzo G, Aiello E, Pietrolucci ME, Arduini D. Are there differences in placental volume and uterine artery doppler in pregnancies resulting from the transfer of fresh versus frozen-thawed embryos through in vitro fertilization. *Reprod Sci* 2016;**23**:1381–1386.

Rousian M, Koster MPH, Mulders A, Koning AHJ, Steegers-Theunissen RPM, Steegers EAP. Virtual reality imaging techniques in the study of embryonic and early placental health. *Placenta* 2018;**64**:S29–S35.

Rousian M, Schoenmakers S, Eggink AJ, Gootjes DV, Koning AHJ, Koster MPH, Mulders A, Baart EB, Reiss IKM, Laven JSE *et al.* Cohort profile update: the Rotterdam Periconceptional Cohort and embryonic and fetal measurements using 3D ultrasound and virtual reality techniques. *Int J Epidemiol* 2021;**50**:1426–1427l.

Saghian R, Bogle G, James JL, Clark AR. Establishment of maternal blood supply to the placenta: insights into plugging, unplugging and trophoblast behaviour from an agent-based model. *Interface Focus* 2019;**9**:20190019.

Schoots MH, Gordijn SJ, Scherjon SA, van Goor H, Hillebrands JL. Oxidative stress in placental pathology. *Placenta* 2018;**69**:153–161.

Senapati S, Wang F, Ord T, Coutifaris C, Feng R, Mainigi M. Superovulation alters the expression of endometrial genes critical to tissue remodeling and placentation. *J Assist Reprod Genet* 2018;**35**:1799–1808.

Steegers-Theunissen RP, Twigt J, Pestinger V, Sinclair KD. The periconceptional period, reproduction and long-term health of offspring: the importance of one-carbon metabolism. *Hum Reprod Update* 2013;**19**:640–655.

Steegers-Theunissen RP, Verheijden-Paulissen JJ, van Uitert EM, Wildhagen MF, Exalto N, Koning AH, Eggink AJ, Duvekot JJ, Laven JS, Tibboel D *et al.* Cohort profile: the Rotterdam Periconceptional Cohort (Predict Study). *Int J Epidemiol* 2016;**45**:374–381.

Stenhouse C, Hogg CO, Ashworth CJ. Associations between fetal size, sex and placental angiogenesis in the pig. *Biol Reprod* 2019;**100**:239–252.

Sun C, Groom KM, Oyston C, Chamley LW, Clark AR, James JL. The placenta in fetal growth restriction: what is going wrong? *Placenta* 2020;**96**:10–18.

Velauthar L, Plana MN, Kalidindi M, Zamora J, Thilaganathan B, Illanes SE, Khan KS, Aquilina J, Thangaratinam S. First-trimester uterine artery Doppler and adverse pregnancy outcome: a meta-analysis involving 55,974 women. *Ultrasound Obstet Gynecol* 2014;**43**:500–507.

Verwoerd-Dikkeboom CM, Koning AH, van der Spek PJ, Exalto N, Steegers EA. Embryonic staging using a 3D virtual reality system. *Hum Reprod* 2008;**23**:1479–1484.

Vogel JP, Chawanpaiboon S, Moller AB, Watananirun K, Bonet M, Lumbiganon P. The global epidemiology of preterm birth. *Best Pract Res Clin Obstet Gynaecol* 2018;**52**:3–12.

Weiss G, Sundl M, Glasner A, Huppertz B, Moser G. The trophoblast plug during early pregnancy: a deeper insight. *Histochem Cell Biol* 2016;**146**:749–756.

Zeve D, Regelmann MO, Holzman IR, Rapaport R. Small at birth, but how small? the definition of SGA revisited. *Horm Res Paediatr* 2016;**86**:357–360.

Zhao L, Sun L, Zheng X, Liu J, Zheng R, Yang R, Wang Y. In vitro fertilization and embryo transfer alter human placental function through trophoblasts in early pregnancy. *Mol Med Rep* 2020;**21**:1897–1909.